Earth Impactors: Orbital Characteristics and Warning Times

Steven R. Chesley* Timothy B. Spahr†

April 10, 2003

1 Introduction

The most important requirement, scientific or otherwise, for any impact mitigation is the recognition of the hazard, since, in the absence of a perceived impact risk, there is neither the incentive nor the capability to address the threat. Therefore, the success of any potential mitigation effort will rely heavily upon our ability to discover, track and analyze threatening objects. In this chapter we will consider the effectiveness of the present surveying and monitoring capabilities by bombarding the Earth with a large set of simulated asteroids that is statistically similar to the impacting population.

Our objective is to determine where on the sky impactors may most readily be detected by search instruments and to evaluate current search techniques for their effectiveness at detecting asteroids on impact trajectories. We also consider the likelihood that existing survey efforts would find previously undiscovered impactors with just weeks to months of warning time. We discuss the factors that affect whether an impactor detection is actually recognized as an NEA discovery and announced to the community for further analysis, including impact monitoring. We close with an example demonstrating how automatic impact monitoring can detect a distant impending impact immediately after discovery, when the impact probability is very low, and how the threat gradually grows more severe during the discovery apparition. In many cases the threat will not be alarming until the object is re-detected at a subsequent apparition. This can substantially diminish the effective warning time, and hence shorten the time available to mitigate the impact.

*Jet Propulsion Laboratory, California Institute of Technology, Pasadena, CA 91109, USA, steve.chesley@jpl.nasa.gov

†Center for Astrophysics, 60 Garden Street,Cambridge, Massachusetts 02138, USA

2 Derivation of Synthetic Impactors

We wish to form a large set of "typical" impactors, and for this purpose we begin with the debiased NEA population model developed by Bottke et al. (2000). Starting with 10^6 values for semimajor axis a, eccentricity e and inclination i that represent the Bottke et al. NEA distribution, we generated approximately 2×10^8 NEAs by adding uniformly distributed longitudes of ascending node Ω and arguments of perihelion ω.

This very large initial NEA set was first reduced to about $58,000$ objects for which the minimum possible orbital separation, or Minimum Orbital Intersection Distance (MOID), is low enough to permit an impact. Specifically, the impact is possible if the MOID is less than the Earth's capture cross section $r_\oplus V_{\rm imp}/V_\infty$, where $r_\oplus$ is the Earth radius, $V_{\rm imp}$ is the impact velocity at the Earth's surface and V_∞ is the encounter or hyperbolic excess velocity. These objects represent the subset of orbits that could impact, but an actual impact also requires that the object's arrival at the minimum distance point be timed to coincide with the Earth's. In this development we call this very low-MOID subset of the NEAs the Potentially Hazardous Asteroids (PHAs), although this is a non-standard usage. According to this definition, the Bottke et al. model predicts about one PHA for every 4000 NEAs.

Because not all of the PHAs are equally likely to impact, we next sampled 1000 impactors from among the PHAs according to the fraction of their orbital period that they spend within the Earth-capture cross section of the Earth's orbit. Deriving the impactors in this way allows for the more hazardous orbital classes, such as low inclination, Earth-like or tangential orbits, to have appropriately increased prominence among the simulated impactors. This *hazard fraction* f is computed by finding the mean anomaly values for which the object enters and exits the toroid formed by the capture cross section surrounding the Earth's orbit. We used the actual Earth orbit, not a circular approximation, for these computations. Values for f in our PHA sample range from as much as a few percent for Earth-like orbits down to 10^{-9} for low-MOID cometary orbits. The hazard fraction is similar to the impact probability per node crossing, and is distinct from, for example, the Öpik (1951) or Wetherill (1967) impact probabilities, which average the impact probability over the precession cycle of the object. Our intent is to measure the hazard posed by a given PHA over a time scale short enough that orbital evolution is not significant, say on the order of a few decades, but even f is probably not ideal for this purpose across the entire range of NEA orbits. In particular, for objects with very low encounter velocities the time spent within the capture cross section torus can be fairly long but this increased risk may be partially offset by a long synodic period. However, the objects for which this concern may be significant comprise

Table 1: Orbital characteristics of NEA subpopulations.

	NEAs (%)	PHAs (%)	Impactors (%)
Shallow Crossers			
Interior ($Q < 1.05$ AU)	1	1	11
Exterior ($q > 0.95$ AU)	8	22	38
Deep Crossers	61	77	53
Atens ($a < 1$ AU)	7	7	23
Low inclination ($< 5°$)	6	25	38
Low V_∞ (< 10 km/s)	–	15	53

only a few percent of our impacting population and we do not believe this plays a significant role in the overall results. Nonetheless, robust techniques for measuring a given orbit's mean impact rate over short time scales are not addressed in the literature and this is an avenue for continued research.

3 Impactor Orbital Characteristics

It is instructive to compare the orbital characteristics of the entire modeled NEA population with those of the PHAs and the impactors. Figure 1 compares the distributions of a, e, i, q and Q, where q and Q are the perihelion and aphelion distances, respectively. From this figure and from Table 1, it is clear that the impacting population has several distinct features. For instance, Earth-similar orbits are prominent among the impactors, as evidenced by the relative excess of impactors with $a \simeq 1$ AU, low e and low i. Indeed, low-inclination orbits are strongly predominant among the PHAs, and even more so among the impactors. We also note that shallow crossing orbits, i.e., those with either q or Q within 0.05 AU of the Earth, have a substantially increased prominence among the impactors. The interior shallow crossers, in particular, have a ten-fold increase in the impacting population, when compared to the entire PHA population.

In general, the encounter velocity V_∞ and impact velocity $V_{\rm imp}$ are significantly greater for PHAs than for impactors. Figure 2 compares the cumulative distributions of impact and encounter velocities between the PHA and impactor sets. The impact velocity, which is a good indicator of the ΔV cost for spacecraft rendezvous (and hence impact mitigation), has a median value that is about 5 km/s less for impactors than for PHAs. This is due to the predominance of low-i shallow-crossing orbits for impactors.

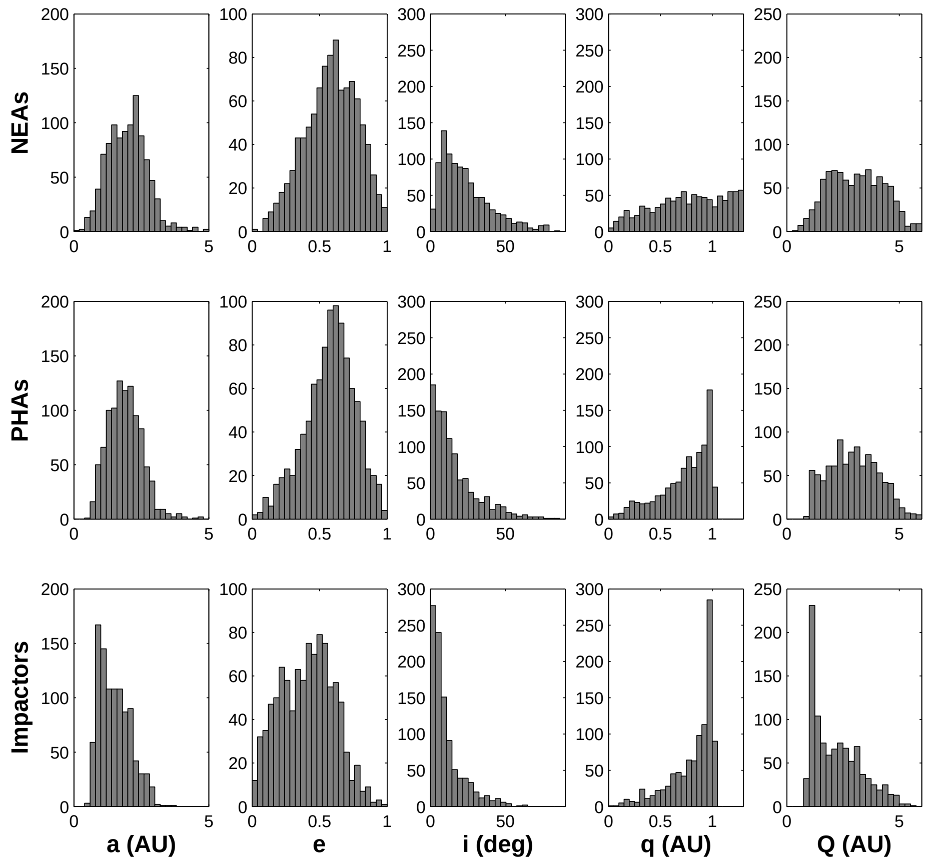

Figure 1: Orbital characteristics of modeled NEAs, PHAs and impactors.

Carusi et al. (2002) describe a simple formula for computing the velocity change required to deflect an asteroid by a given distance within a specified time interval. Using their approach, we can compute the required Δv to deflect each impactor by one Earth radius as a function of lead time. Taking the geometric mean of these values we find the relation

$$\Delta v = \frac{0.035 \text{ m/s}}{T},$$

where T is the number of years before impact that the impulse is applied. This is half the value offered by Ahrens and Harris (1994), an excellent agreement considering the disparate approaches involved and that the dispersions around this geometric mean are more than an order of magnitude.

We do not attach individual sizes to our set of synthetic impactors according

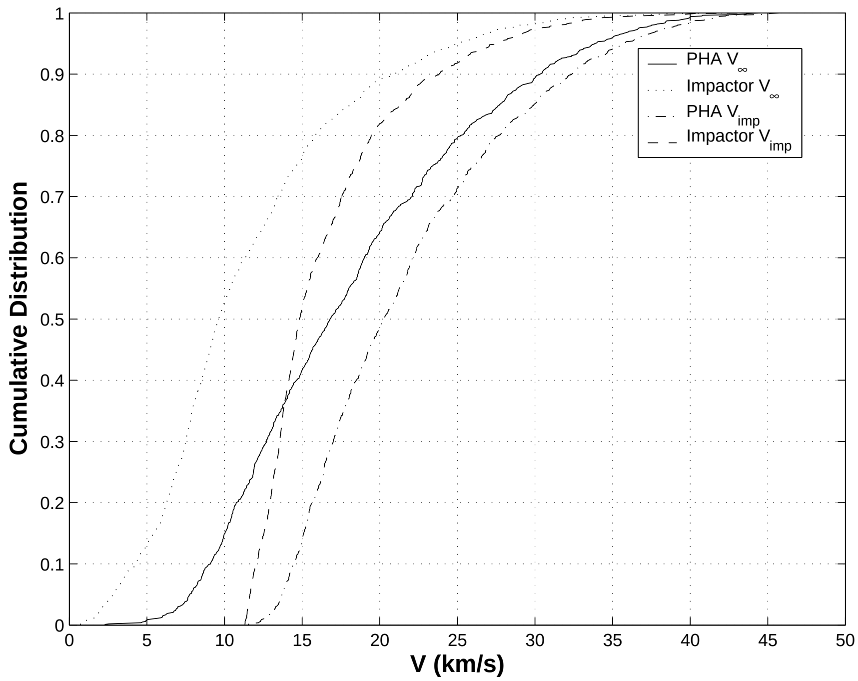

Figure 2: Cumulative distributions of impact velocity V_{imp} and encounter velocity V_∞ for the PHA and impactor sets. The impact velocity is a simple function of the Earth escape velocity ($V_e \simeq 11.2\ \mathrm{km/s}$) and the encounter velocity: $V_{\mathrm{imp}}^2 = V_\infty^2 + V_e^2$.

to some expected size frequency distribution, but instead we shall assume that all have the same absolute magnitude. For this assumption to be meaningful we have to accept the hypothesis that there is no correlation between physical size and orbit among the NEAs, so the synthetic impactor set represents the true impactor population, no matter the size. Thus, with this approach, we assume that our impactors are statistically similar to the real impactor population at a given size or in a given size range.

4 Impactor Observability

With our impactors in hand, we wish to see how and where they are observable in the decades leading up to collision. To answer this question, we selected the LINEAR Experimental Test Site (ETS), near Socorro, New Mexico, as the observing location. We consider an object observable if it is situated at least 60° from the Sun, with proper motion in the range 0.05–$10.0^\circ/\text{day}$ and at no more than 3 air masses. Furthermore, it must be brighter than the detection limit of the survey telescope.

The question of whether an object is bright enough for detection depends upon both its assumed intrinsic brightness and the survey's assumed limiting magnitude, or depth. In preparing the ephemerides, we only need to calculate the difference between the apparent visual magnitude and the absolute magnitude, $S = V - H$. Then, given an assumed absolute magnitude H and survey limiting magnitude V_{lim}, the object is considered bright enough to be detected if $S + H < V_{lim}$, or equivalently if $S < V_{lim} - H$. For this report, we will vary the assumed H, while assuming a survey depth of $V_{lim} = 20$ throughout. This allows us to frame our results in terms of absolute magnitude, rather than the much less intuitive $V_{lim} - H$. It also means that any of these results can be applied to a different survey depth simply by incrementing or decrementing the quoted H-value by the corresponding change from $V_{lim} = 20$.

Figure 3 indicates the sky-plane density of the 1000 impactors over the 100-year period leading up to impact. The plot indicates clearly that, for a $V_{lim} = 20$ survey, the most favorable region to search for $H = 18$ impactors is near the ecliptic between solar elongations of 60° and 90°. There is also a modest concentration at opposition because objects are brightest at full phase. On the other hand, the peaks away from opposition at low elongations are present because the sky density of objects is much higher as we look through the "belt" of impactors. However, as the elongation becomes smaller the increasing density of objects is eventually overcome by the decreasing brightness due to phase losses. These phase losses are more significant for smaller objects, and the corresponding plot (not shown) for $H = 20$ shows the peaks at low elongations are less substantial than the opposition peak. For $H = 22$, these peaks are no longer significant.

Another approach to plotting the sky density of impactors is to weight them according to their likelihood of collision. In other words, instead of weighting all objects equally when accumulating the results, we can weight them according to the hazard fraction f described in Sec. 2. The result of this alternate approach, which can be thought of as mapping impact probability onto the sky, is presented in Figure 4 for the same data set used in Fig. 3. The results indicate clearly that the *hazard*-density approach even further favors the low-elongation regions over the opposition region, as compared to the *object*-density plots. Indeed, using this approach, the prime discovery region for hazardous objects is situated predominantly at low elongations for sizes as small as $H = 22$.

For various reasons, searching the near-sun region is more operationally challenging than searching near opposition, where present survey efforts have been

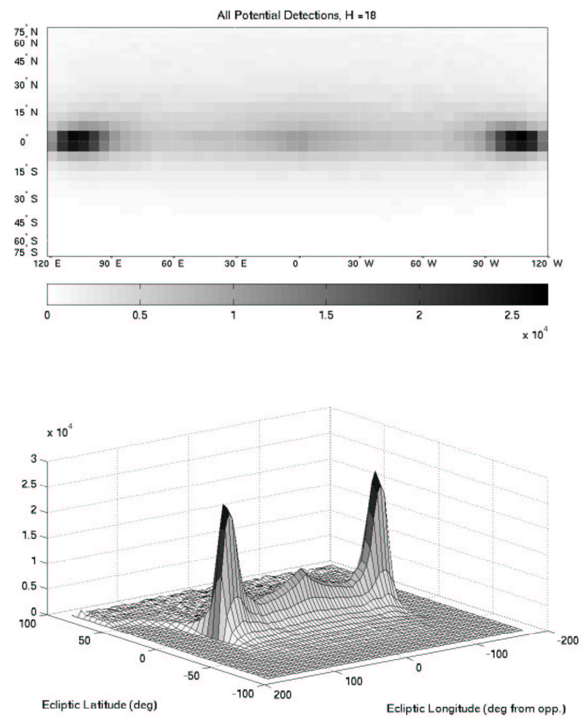

Figure 3: Sky-plane distribution of $H = 18$ impactors at LINEAR's ETS, assuming a survey depth of $V_{lim} = 20$. In the top diagram, the origin is the solar opposition point.

concentrated. Also, current survey strategies are tailored towards fulfilling the Spaceguard goal of finding all NEAs larger than 1 km in diameter, and searches for NEAs, as opposed to impactors, are clearly the most productive around opposition since so many NEAs are of the Amor class, with orbits completely exterior to the Earth's. On the other hand, a search for large impactors is not expected to find such an object over human timescales, simply because large impacts are so rare. If a large NEA *is* set to impact the Earth in the next century it will most readily be detected far from opposition, as we show in the next section.

5 Survey Simulations

Given our set of impactors, one can ask whether and when they would be discovered by various NEO surveys with differing sky coverages and limiting magnitudes.

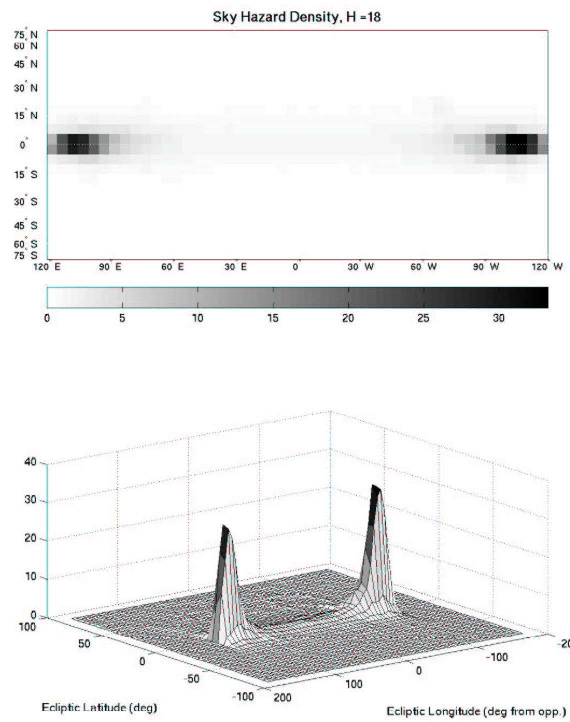

Figure 4: Sky-plane distribution of impactor hazard. Same as Fig. 3, except the residence times in each bin are weighted according to the associated hazard fraction f for that object.

To consider these questions, we simulated two fictitious NEO surveys over the century prior to impact. The first survey, dubbed "OPPOSITION," is based loosely on the strategy and capability of the LINEAR system (Stokes et al., 2000), the world's most prolific discoverer of NEOs. OPPOSITION covers the ecliptic and opposition regions heavily with modest coverage at higher ecliptic latitudes, but no coverage at solar elongations less than 90°. The survey model assumes 75% clear weather and some down time due to lunar interference. Figure 5 indicates the distribution of the mean time between detection by OPPOSITION for the synthetic impactors at various sizes. We note from this chart that the mean time between detection for most impactors larger than $H = 20$ will be a few decades or less.

Another interesting result that can be extracted from the data is the detection lead time. Figure 6 depicts the fraction of impactors that were serendipitously detected by OPPOSITION before impact as a function of the time until impact and

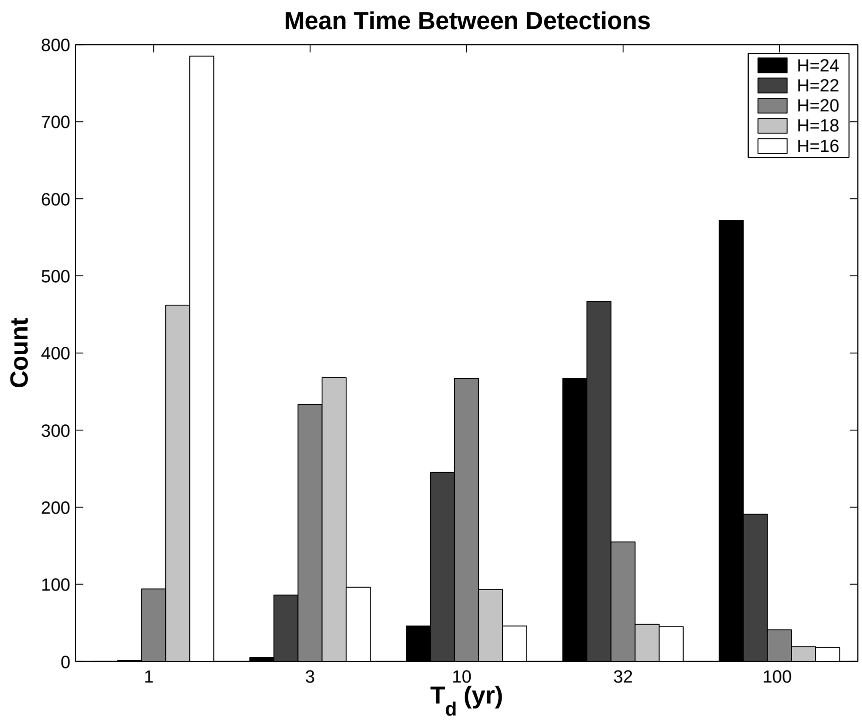

Figure 5: Histogram of mean time T_d between detections (not discoveries) for impactors at various absolute magnitudes, for the OPPOSITION survey. Objects that escaped detection over the entire simulation are included in the 100-year bin.

as a function of absolute magnitude. For example, the plot indicates that 48% of $H = 24$ impactors will be detected sometime in the century leading up to impact, and that only 20% will be detected in the last year before impact. Similarly we can see that, for $H = 20$ objects, about a third will be serendipitously detected in the last month before impact, whereas 12% will be detected only in the last week before impact. Differencing these two numbers tells us that roughly 20% of previously undiscovered $H = 20$ impactors will be detected by OPPOSITION with 1–4 weeks of warning time, which, in principle, could be sufficient to mount an effective evacuation of the impact region or threatened coastal regions.

Figure 6 also indicates that OPPOSITION would only detect 98% of objects, no matter the size. This is because the survey never looks beyond 90° from opposition and some shallow-crossing interior objects rarely enter the search region. To further consider this point we tested a second survey strategy, with equipment and

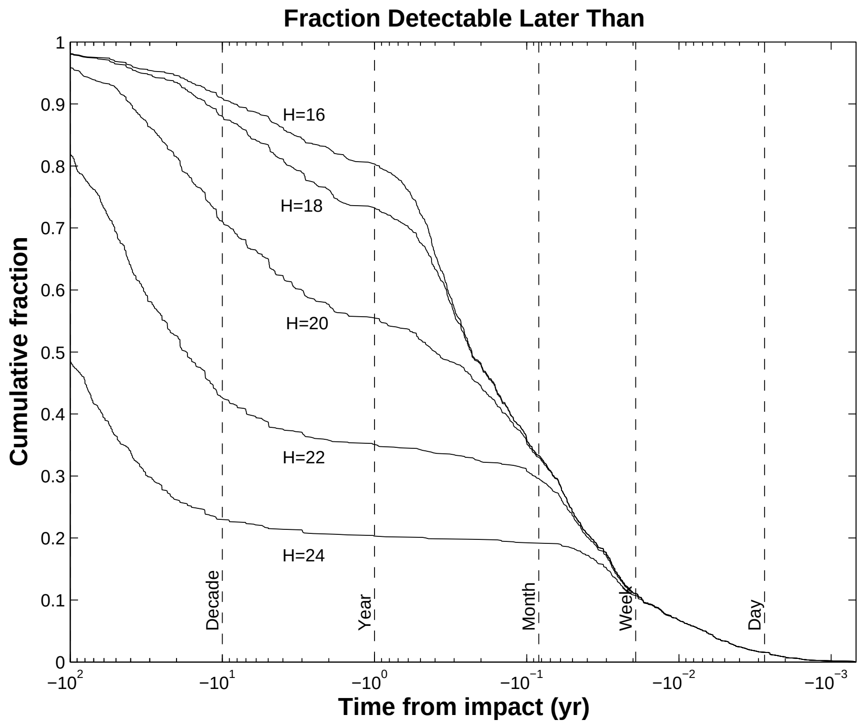

Figure 6: The fraction of impactors serendipitously detected later than a given time before impact, for the OPPOSITION survey.

location similar to OPPOSITION. However, this survey, which we call "NEAR-SUN," never searches near the opposition region, instead concentrating exclusively on the high density regions indicated in Figs. 3 & 4. Specifically, NEAR-SUN trolled for impactors within $15°$ of the ecliptic and at solar elongations ranging from $60°$ to $110°$. Figure 7 compares the two surveys' impactor completeness as a function of time prior to impact for several different impactor sizes. From that plot it is clear that NEAR-SUN beats OPPOSITION at detecting large impactors ($H \leq 18$), especially when the completeness exceeds 80%. But for smaller objects the phase losses prevent NEAR-SUN from discovering objects as rapidly.

We can measure survey completeness by the number of objects detected, as in Fig. 7, or by the percentage of the aggregate impact flux detected, in much the same way as Fig. 4 projected the risk onto the sky. The result of this approach is given in Fig. 8, where we can see that, despite its rather limited sky coverage, NEAR-SUN is markedly better at detecting the most hazardous large impactors, even excelling

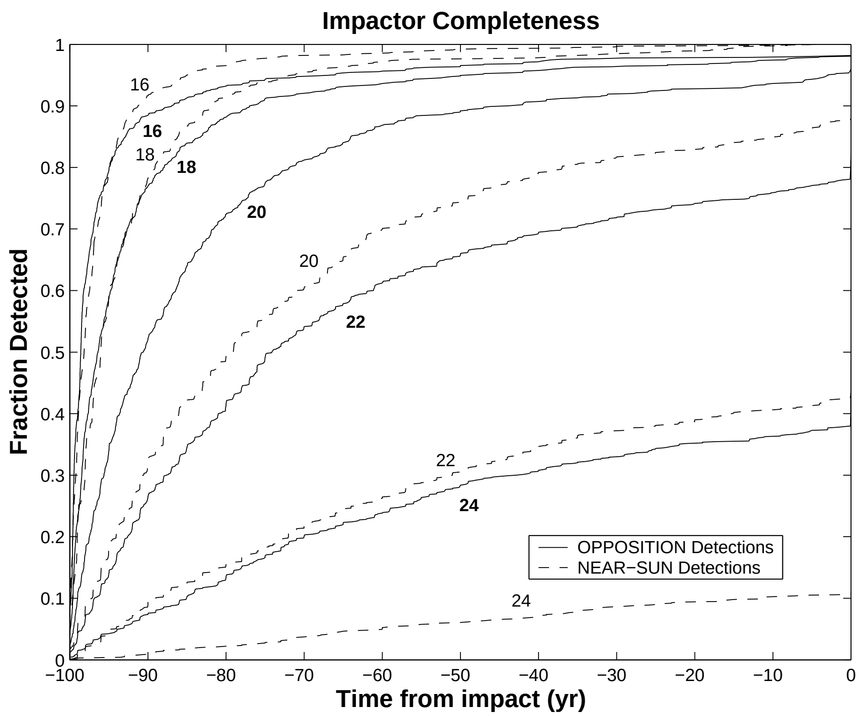

Figure 7: Comparison of OPPOSITION and NEAR-SUN survey performance, in terms of impactor completeness. Each curve is labeled with the assumed absolute magnitude.

as faint as $H = 20$. Note also that the 2% of impactors that went undetected by OPPOSITION during the 100-year simulation actually comprised about 6% of the hazard. This is because the interior shallow-crossing objects that were missed hold a disproportionate share of the aggregate impact risk.

The obvious conclusion from these results is that the near-sun region should not be neglected when searching for large impactors. Given, however, that this region of sky is only observable for a few hours each morning and evening, the remaining telescope time could be used for an opposition-type survey, thus concentrating on the two most productive areas of sky to survey for the most hazardous objects. Note also that the size results given in this section are for a survey depth of $V_{lim} = 20$. For a fainter survey, the absolute magnitudes need to be adjusted fainter accordingly. For example, if we extend the survey to $V_{lim} = 24$, the proposed limit of the recently announced Pan-STARRS project (Kaiser and Pan-STARRS Team, 2002),

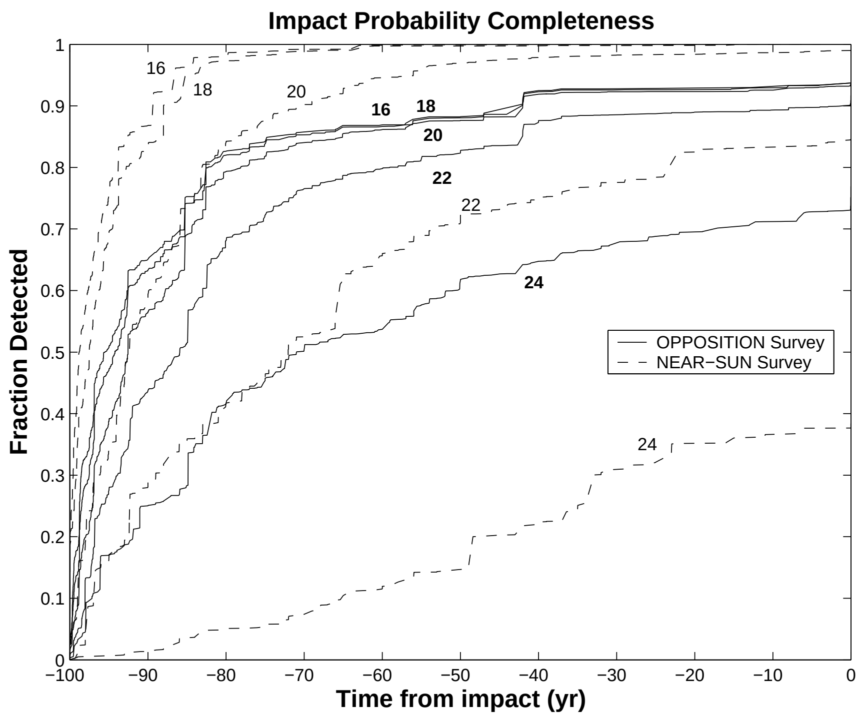

Figure 8: Comparison of OPPOSITION and NEAR-SUN survey performance, in terms of impact hazard completeness. Each curve is labeled with the assumed absolute magnitude.

then we can use the $H = 20$ curves of Fig. 8 (for $V_{lim} = 20$) to represent the case where $H = 24$ and $V_{lim} = 24$. Thus the figure indicates that for Pan-STARRS the NEAR-SUN strategy would be more effective than the OPPOSITION strategy for all sizes of interest.

6 Warning Time: Post-Detection Issues

The detection lead time is important in determining the time available for mitigation, but it is not the only factor. There are several hurdles to be crossed before a detection is announced to the community as a discovery. The first among these is the recognition that an object has unusual motion (Jedicke, 1996). If a survey makes this determination it calls out the detection when forwarding the data to the Minor Planet Center (MPC). If the MPC staff agrees with the assessment then it is placed on the WWW NEO Confirmation Page for verification by other observers. If the object is followed and confirmed to be an NEA then the MPC will issue a discovery announcement. At any of these steps a potential impactor detection could be scrapped, and thus escape discovery. It is well known that this actually happens, but it is difficult to discern the extent to which these factors delay discovery of NEAs.

There is also some delay between the discovery of the asteroid and the recognition that it poses a threat worthy of mitigation. The idea of continually monitoring the ever-evolving asteroid orbit catalog for possibilities of impact is fairly new, and the first automatic collision monitoring system was fielded less than three years ago. Today there are two independent and parallel systems, Sentry[1] at JPL and NEODyS[2] at the Univ. of Pisa, that are operating continuously to scan for potential impacts. These efforts have been successful at detecting potentially hazardous future encounters for newly discovered asteroids and reporting the results to the NEO community. Follow-up observers have responded enthusiastically with observations that permit the hazard assessment to be refined and usually eliminated.

We close with a case study of the rate at which the probability of an impending impact increases after discovery, and we examine how this can affect the lead time for mitigation. We have selected a typical impactor on a shallow-crossing exterior orbit with moderate inclination (Table 2). It impacts the Earth on Feb. 26, 2000. For this example we assume $H = 22$ and that the object is discovered at the second apparition before impact, in Dec. 1983. With only the three-day discovery data arc the actual impact is detected by Sentry (at a probability of 2×10^{-7}), along with many other spurious impact possibilities. (Here we use the term "spurious" to indicate a potential impact detection that will eventually be eliminated with more data, rather than to indicate that the detection is somehow incorrect or erroneous.) Among these early spurious potential impacts is one occurring on the same day as the true one. Such cases typically indicate a relationship, described by the theory of interrupted returns (Milani et al., 2002), between the two dynamically distinct potential impact trajectories.

Figure 9 depicts the impact probabilities for both of these potential impacts as a function of the observed arc length. The behavior of the spurious potential impact is typical of cases seen to date: The impact probability rises as long as the Earth remains within a collapsing uncertainty region, until eventually the uncertainty region shrinks to the point that it no longer encompasses the Earth, at which point the impact probability falls steeply. In this case, the probability reaches a peak of 2×10^{-4} with three weeks of data and is completely eliminated less than three

[1] `http://neo.jpl.nasa.gov/risk`
[2] `http://newton.dm.unipi.it/neodys`

Table 2: Full Precision Orbital Elements for Simulated Impactor.

Quantity	Value
Epoch	2000-01-27.64180445 TDT
a	1.92551764232665 AU
e	0.506153768512869
Ω	$337.350228048783°$
ω	$151.900629508322°$
i	$11.5131345762734°$
M	$-2.90435767774188°$

weeks later. In contrast, the true impact's probability increases steadily during the discovery apparition until the object is lost in the daytime sky, with more than six months of observations. The impact probability stands at 7% at the end of the discovery apparition and the impact is less than 16 years away. The impact is confirmed 4 years later when the object is recovered at the next observing opportunity. At this point only 11 years remain until impact.

Two impact hazard scales are in regular use, the Torino Scale (Binzel, 2000), which is intended for public communications, and the Palermo Technical Scale (Chesley et al., 2002), which is tailored to facilitate communication among specialists. The time history of these two scale values is also depicted in Fig. 9 for this simulation. We remark that the spurious impact detection did reach a Torino Scale value of 1 before beginning its decline, which is not unusual. We also note that the true impact event was rated positive on the Palermo Scale after only 68 days of observation. A positive Palermo Scale value indicates that the event is more threatening than the average impact flux for objects in the size range $H < 22$. As is typical of impacts occurring a few decades into the future, the Torino Scale rating exited the "1" region, in this case moving into the "3" region, at about the same time that the Palermo Scale became positive. During the four years that the simulated impactor was unobservable the Palermo Scale stood at $+0.74$, which is greater than the highest real-world value computed to date ($+0.38$ for 2002 NT_7). This exercise raises the question as to what might be done to prepare for the potential impact during the years when the impact is not confirmed but the object is unobservable.

We face a similar but less severe situation even now, with the object 1997 XR_2. This asteroid, which at $H = 20.8$ is approximately 230 meters in diameter, was heavily observed for 28 days at its discovery apparition in late 1997. With this

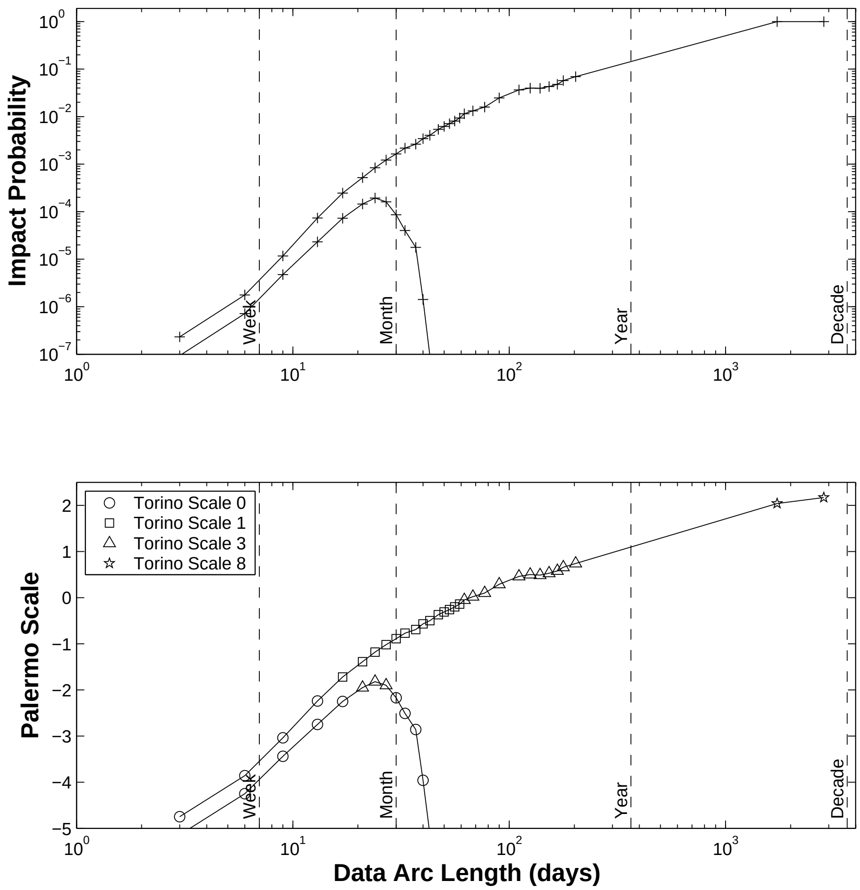

Figure 9: For the simulated impactor outlined in the text, with orbital elements given in Table 2, these plots present the computed impact probability (top) and Palermo/Torino Scale values (bottom) as a function of the data arc length used in the orbit determination process.

data set the JPL Sentry system reports two potential impacts in the year 2101, each rating Torino Scale 1 and with impact probabilities around 5×10^{-5}. This asteroid is expected to be recovered at its next observing opportunity in 2006-2007, at which point the possibility of impact will either be confirmed or (more likely) eliminated. Incidentally, this object would almost certainly have been observed far longer at the discovery apparition in 1997-1998 had the potential impacts been recognized at the time, but, unfortunately, the first automatic monitoring system was then still several years away.

7 Conclusions

This chapter describes our work to characterize the orbits and observability of Earth impacting asteroids and to understand the factors affecting the impact warning time. We summarize the major conclusions with the following remarks.

- The orbital distribution of the impacting population is noticeably different from the general low-MOID population, with an increased presence of low-i orbits, shallow-crossing orbits and low-V_∞ orbits.

- Statistically, the impacting population will collide with Earth at lower relative velocities than the general PHA population. Since the impact velocity is a rough indicator of the spacecraft ΔV costs to effect a rendezvous, impactors should be more accessible for spacecraft mitigation attempts than objects in the general PHA population.

- Surveys will most readily detect impactors for which $H < V_{lim}$ in two fairly small "sweet spots" situated within 15° of the ecliptic and 90–120° from opposition. Fainter objects will be preferentially found in the opposition region.

- Among the impacting population, those most prone to impact are predominantly concentrated around the sweet spots if $H < V_{lim} + 2$. Surveys that concentrate on these regions reduce the risk of large impacts significantly faster than opposition-style surveys.

- A LINEAR-like survey would detect roughly 20% of previously undetected $H = 20$ impactors with 1–4 weeks of warning time, which in some cases may be enough time to mount an effective evacuation of affected areas.

- After its initial detection by a survey there are a series of hurdles that an impactor must cross before its hazard can be appreciated. If the objects does make the leap from detection to discovery then automated impact monitoring systems can be expected to detect the impending impact very quickly. However, for impacts some decades in the future, the statistical hazard associated with the impact detection may remain fairly modest for months following the discovery. Depending upon the observing circumstances, this delay in recognition may trim several years from the time that could be dedicated to averting the impact.

Acknowledgments

The authors are grateful to Alessandro Morbidelli, who provided one million NEA orbits based upon the Bottke et al. (2000) population model, Alan Harris, who contributed important insight through various discussions and lectures, and Don Yeomans for his helpful review of this manuscript. This research was conducted in part at the Jet Propulsion Laboratory, California Institute of Technology, under a contract with the National Aeronautics and Space Administration.

References

Ahrens, T. J. and Harris, A. W. (1994). Deflection and Fragmentation of Near-Earth Asteroids. In Gehrels, T., editor, *Hazards Due to Comets & Asteroids*, pages 897–927. Univ. Arizona Press, Tucson.

Binzel, R. P. (2000). The Torino Impact Hazard Scale. Planet. Space Sci., 48:297–303.

Bottke, W. F., Jedicke, R., Morbidelli, A., Petit, J., and Gladman, B. (2000). Understanding the Distribution of Near-Earth Asteroids. *Science*, 288:2190–2194.

Carusi, A., Valsecchi, G. B., D'Abroam, G., and Boattini, A. (2002). Deflecting NEOs in route of collision with the earth. *Icarus*, 159:417–422.

Chesley, S. R., Chodas, P. W., Milani, A., Valsecchi, G. B., and Yeomans, D. K. (2002). Quantifying the risk posed by potential Earth impacts. *Icarus*, 159:423–432.

Jedicke, R. (1996). Detection of Near Earth Asteroids Based Upon Their Rates of Motion. AJ, 111:970–982.

Kaiser, N. and Pan-STARRS Team (2002). The Pan-STARRS optical survey telescope project. BAAS, 34:1304.

Milani, A., Chesley, S. R., Chodas, P. W., and Valsecchi, G. B. (2002). Asteroid close approaches: Analysis and potential impact detection. In Bottke, W. F., Cellino, A., Paolicchi, P., and Binzel, R. P., editors, *Asteroids III*. Univ. Arizona Press, Tucson. in press.

Öpik, E. J. (1951). Collision probability with the planets and the distribution of planetary matter. *Proc. R. Irish Acad. Sect. A*, 54:165–199.

Stokes, G. H., Evans, J. B., Viggh, H. E. M., Shelly, F. C., and Pearce, E. C. (2000). Lincoln Near-Earth Asteroid Program (LINEAR). *Icarus*, 148:21–28.

Wetherill, G. W. (1967). Collisions in the asteroid belt. J. Geophys. Res., 72:2429–2444.